UCRL-ID-123893

Crosshole EM for Oil Field Characterization and EOR Monitoring: Field Examples from Lost Hills, California

Michael Wilt, Clifford Schenkel, Michael Wratcher,
Ilia Lambert, Carlos Torres-Verdin, and Hung-Wen Tseng

July 16, 1996

Lawrence Livermore National Laboratory

This is an informal report intended primarily for internal or limited external distribution. The opinions and conclusions stated are those of the author and may or may not be those of the Laboratory.

Work performed under the auspices of the U.S. Department of Energy by the Lawrence Livermore National Laboratory under Contract W-7405-ENG-48.

DISCLAIMER

This document was prepared as an account of work sponsored by an agency of the United States Government. Neither the United States Government nor the University of California nor any of their employees, makes any warranty, express or implied, or assumes any legal liability or responsibility for the accuracy, completeness, or usefulness of any information, apparatus, product, or process disclosed, or represents that its use would not infringe privately owned rights. Reference herein to any specific commercial product, process, or service by trade name, trademark, manufacturer, or otherwise, does not necessarily constitute or imply its endorsement, recommendation, or favoring by the United States Government or the University of California. The views and opinions of authors expressed herein do not necessarily state or reflect those of the United States Government or the University of California, and shall not be used for advertising or product endorsement purposes.

This report has been reproduced
directly from the best available copy.

Available to DOE and DOE contractors from the
Office of Scientific and Technical Information
P.O. Box 62, Oak Ridge, TN 37831
Prices available from (615) 576-8401, FTS 626-8401

Available to the public from the
National Technical Information Service
U.S. Department of Commerce
5285 Port Royal Rd.,
Springfield, VA 22161

Crosshole EM for Oil Field Characterization and EOR Monitoring: Field Examples from Lost Hills, California

Michael Wilt, Clifford Schenkel, Michael Wratcher,
Ilia Lambert, Carlos Torres-Verdin, and Hung-Wen Tseng

July 16, 1996

Crosshole EM for Oil Field Characterization and EOR Monitoring: Field Examples from Lost Hills, California

Michael Wilt and Clifford Schenkel
Lawrence Livermore National Laboratory

Michael Wratcher and Ilia Lambert
Mobil Development and Production U.S.

Carlos Torres-Verdin
Schlumberger-Doll Research

Hung-Wen Tseng
University of California at Berkeley

Abstract

A steamflood recently initiated by Mobil Development and Production U.S. at the Lost Hills #3 oil field in California is notable for its shallow depth and the application of electromagnetic (EM) geophysical techniques to monitor the subsurface steam flow. Steam was injected into three stacked eastward-dipping unconsolidated oil sands at depths from 60 to 120 m; the plume is expected to develop as an ellipsoid aligned with the regional northwest–southeast strike. Because of the shallow depth of the sands and the high viscosity of the heavy oil, it is important to track the steam in the unconsolidated sediments for both economic and safety reasons.

Crosshole and surface-to-borehole electromagnetic imaging were applied for reservoir characterization and steamflood monitoring. The crosshole EM data were collected to map the interwell distribution of the high-resistivity oil sands and to track the injected steam and hot water. Measurements were made in two fiberglass-cased observation wells straddling the steam injector on a northeast–southwest profile. Field data were collected before the steam drive, to map the distribution of the oil sands, and then 6 and 10 months after steam was injected, to monitor the expansion of the steam chest. Resistivity images derived from the collected data clearly delineated the distribution and dipping structure of the target oil sands. Difference images from data collected before and during steamflooding indicate that the steam chest has developed only in the middle and lower oil sands, and it has preferentially migrated westward in the middle oil sand and eastward in the deeper sand.

Surface-to-borehole field data sets at Lost Hills were responsive to the large-scale subsurface structure but insufficiently sensitive to model steam chest development in the middle and lower oil sands. As the steam chest develops further, these data will be of more use for process monitoring.

Introduction

For a number of years, heavy oil has been produced with the aid of steam injection from shallow unconsolidated sands in the San Joaquin Valley of central California. Although most thermal enhanced oil recovery (EOR) projects have been economically successful, many have problems of steam override, steam bypass, and inefficient sweep as a result of channeling. Thus, developing low-cost geophysical monitoring methods for EOR has been a priority of operating companies for some time. Seismic techniques have been applied to EOR monitoring with good success, but the high cost of drilling dedicated observation wells and doing surveys deters many developers (Eastwood et al., 1994). Lower-cost alternative techniques are continually being sought to make further use of observation wells and allow greater sensitivity to produced and injected fluids.

Electromagnetic techniques, which are sensitive to the subsurface electrical resistivity, are responsive to changes in the rock pore fluids. This contrasts with the seismic techniques, which have higher sensitivity to the rock matrix. EM techniques are therefore ideal for monitoring EOR processes because of the large-scale fluid and heat flow. Traditionally, however, EM techniques have been employed only in borehole logging. Only recently have instrumentation and interpretation techniques become available for crosshole and surface-to-borehole EM configurations.

Borehole induction logging measurements in oil fields undergoing EOR confirm the high sensitivity of electrical resistivity to changes in subsurface temperature and pore fluid. Published reports have shown that the resistivity typically decreases from 35 to more than 80% after steam injection (Mansure and Meldau, 1990; Ranganayaki et al., 1992; Spies and Greaves, 1990). This decrease occurs because temperature increases and because the high-resistivity oil is replaced by the lower-resistivity steam and water injectate mixture. If the resistivity distribution can be determined between wells, then the field engineer would have a powerful tool for tracking injected fluids and thereby controlling the recovery process.

This short case history illustrates the application of crosshole and surface-to-borehole EM methods for reservoir characterization and EOR monitoring at the Lost Hills oil field in central California. The Tulare 3T steamflood at Lost Hills is among the shallowest on record; steam injection occurs at depths of less than 60 m. It is therefore most important to monitor the flow for safety as well as economic reasons. The EM method was chosen as a pilot technology to monitor the steamflood because of the high sensitivity of measurements to regions affected by underground steam.

This project was initiated from discussions between Ranga Ranganayki at Mobil Research and Michael Wilt at Lawrence Livermore National Laboratory (LLNL) in 1990. The field operators at Mobil Lost Hills became involved with the onset of field activities in 1991. Much of the technical work was accomplished through the crosshole EM

consortium, which includes Mobil, Schlumberger-Doll Research, LLNL, Lawrence Berkeley National Laboratory (LBNL), and the University of California at Berkeley.

Geologic Setting

The Lost Hills oil field is located along the crest of the Lost Hills anticline in California's San Joaquin Valley. This anticline is the southernmost segment of a northwest-trending segmented antiform that includes the Kettleman Hills anticlines and the Coalinga anticline to the north. It is located on the western margin of the San Joaquin Basin and roughly parallels the trace of the San Andreas fault zone 20 miles to the west (Figure 1). The San Andreas system is thought to be the dominant control for structure in the western San Joaquin Valley oil fields (Miller et al., 1990).

The Lost Hills oil field was discovered in 1911, although substantial production did not occur until the mid to late 60s. Presently, oil is produced via steam and water flooding from a series of stacked oil sands ranging from the Miocene Monterey shales and diatomites to the Pleistocene Tulare sands.

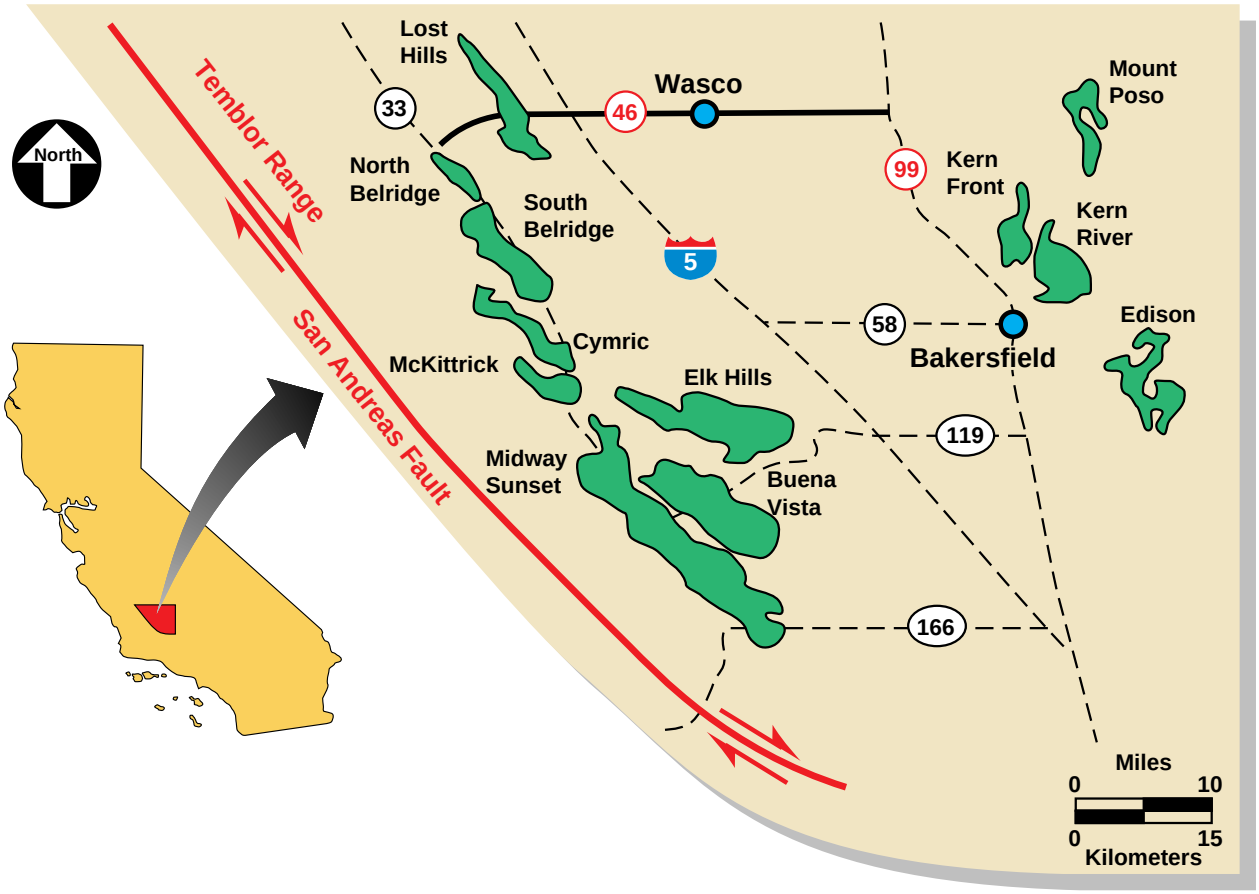

Figure 1. Site location map for the Lost Hills oil field.

The Tulare Formation records the Pleistocene history of basin filling in the present-day San Joaquin Valley. It is the first nonmarine deposit to be preserved, unconformably overlying the marine Pliocene / Miocene Etchegoin Formation (Figure 2). The unconformity at the base of the Tulare is angular and therefore at least in part tectonic in nature. Although the underlying units contain numerous normal faults, the Tulare is largely unfaulted and has apparently filled in the older faulted eroded surface.

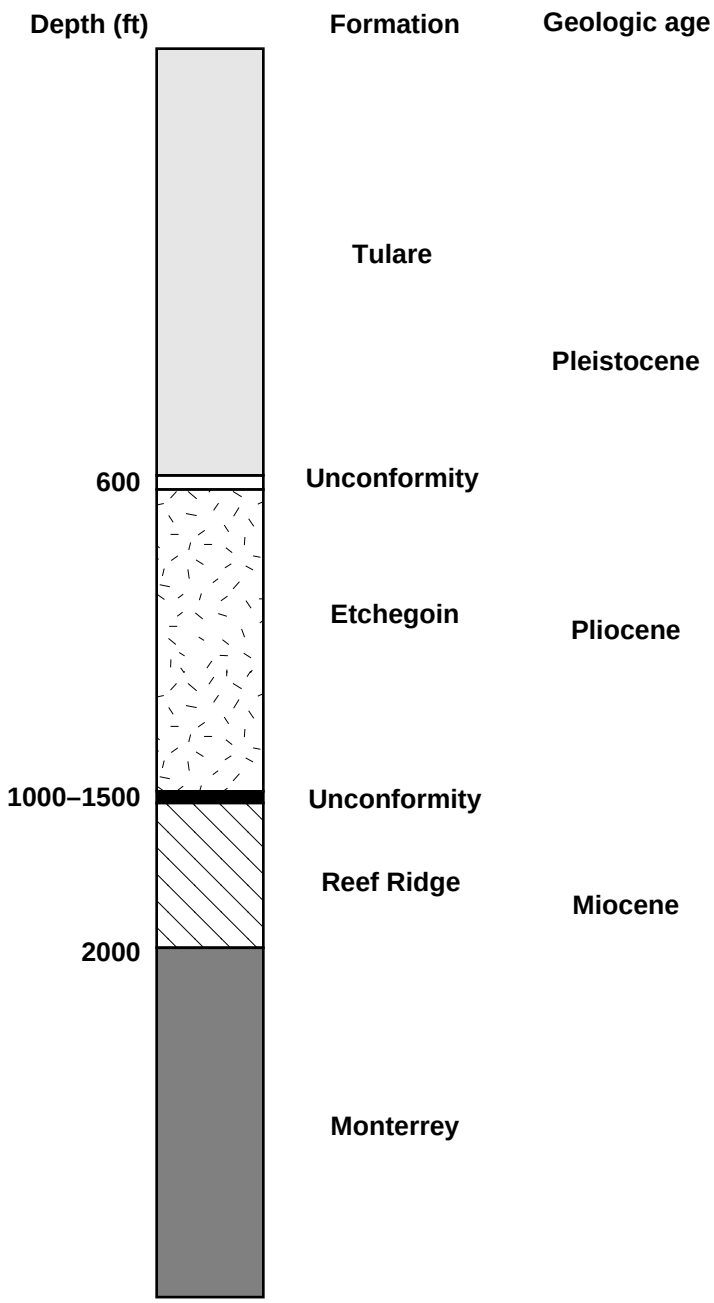

Figure 2. Composite stratigraphic column for the Lost Hills field.

The Tulare records small- to medium-sized streams depositing loads in lacustrine delta complexes at the western margin of Pleistocene Lake Corcoran. Because of the system's high energy, there are abundant clean sands throughout the field. Clay content is highly variable, depending on the facies type. Sand geometry is complicated but can generally be thought of as a series of discontinuous sheets and troughs. Well correlations must take into account the highly transitory depositional environment. Also, sedimentary packages can change dramatically within one steam pattern with a large resulting impact on fluid flow.

Permeabilities range from a few hundred millidarcies in muddy sands to between 1000 and 3000 millidarcies in the clean sands. The total porosity ranges from 38 to 42% and displays little variability. Oil saturations range between 35 and 75% with a weighted average of 65%. The oil produced from Tulare sands is biodegraded and water washed; it ranges from 10 to 13 API gravity (Miller et al., 1990).

Steamflood Design

Initial steamflooding activities at Lost Hills #3 were targeted in the Etchegoin sands, with a line-drive steamflood in the late 1980s. The shallow Tulare section was targeted in the 1991 steamflood development termed the 3T. With a structural dip of approximately 5 degrees and an initial reservoir pressure of 35 psig, the Tulare has minimal reservoir energy to drive production. Recovery via primary and cyclic steam depletion in adjacent properties is 12% of the oil in place (OOIP). In contrast, steamflooding is expected to increase the ultimate recovery to 55% OOIP.

The 3T steamflood was designed using the nearby 3B Tulare steamflood, with 4-acre (16 km^2) inverted 7 spot patterns, as a model for optimization (Figure 3). The 3T design incorporates the same number of wells per pattern to deplete a larger area, approximately 5 acres (20 km^2). By using a larger spatial pattern, we hoped to reduce the capital investment required for the project. What was not foreseen is that a low allowable injection pressure (0.6 psi / ft) coupled with shallow injection depths (50 m average) restricts injectivity to rates below what is required for efficient recovery on this larger pattern.

Yet another critical challenge at 3T is the existence of undersaturated zones (air gaps) within the oil column. These regions act as "thief" zones, transporting injected steam into other patterns or to overlying air sands. The 3T steamflood is located just eastward from known Tulare undersaturated zones. While this location prevents initial thieving of heat, if the steam chest connects to the existing undersaturated zones, it will migrate preferentially westward and much of the pressure will be lost.

The Tulare is divided into the upper, middle, and lower flow units. The units are accessed via limited entry injectors, designed to flood each with 1.15 bspd / net acre-ft. Although the steamflood was initiated in 1991, initial steam injectivity was very low

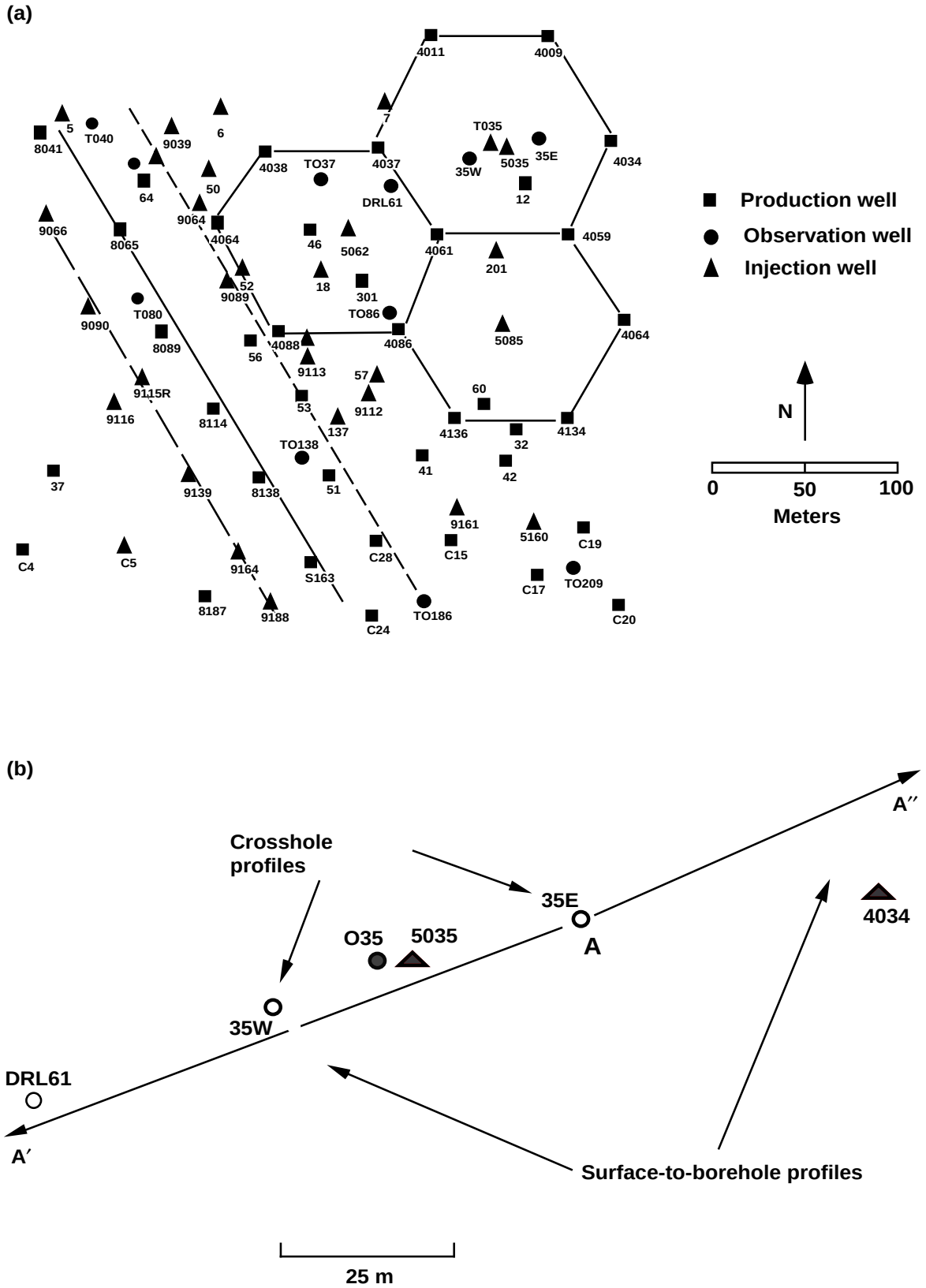

Figure 3. Site map for the EM project at the Lost Hills 3T steamflood.

because of the high oil saturations with low mobility (cold oil). Intense producer cyclic steaming has been required to supplement pattern heat.

The pattern under EM surveillance is one of two surviving patterns. It, too, has had continuous injection into the upper Tulare via injector #5035 since 1991, but at very low rates. In late 1993, we increased the injection rate by steam fracturing #5035 and by recompleting a nearby service well, TO-35, into an injector for the middle and lower Tulare zone. At present, 450 bbl / day is injected into the primary and secondary steam-injection wells. Production response to the steam injection occurred, finally, in February 1995.

Objectives of the EM Surveillance

The northeastern most of four 3T pilot patterns was selected for monitoring with crosshole and surface-to-borehole EM. We wanted to determine if the EM measurements were effective in locating steam-saturated zones and if they could provide information on steam flow before the temperature fronts arrived at observation or production wells. In addition, we wanted to determine the value of interpreted EM sections in defining sand body continuity.

The crosshole surveys are designed to examine flow in the plane between the boreholes and to track sand-bed continuity. This method is quite sensitive to subsurface flow in individual layers. The surface-to-borehole surveys were designed to investigate upward-moving steam flow and flow outside the plane between observation wells 35E and 35W. We expect that these measurements will have a lower resolution than the crosshole data and may not have sufficient sensitivity to detect deep-seated resistivity changes due to steam flow. The advantages of this method are that it does not require two boreholes and that the images are not limited to the plane between wells.

Basic Principles of Crosshole EM

A simplified EM system consists of a transmitting magnetic dipole (loop) antenna broadcasting a sinusoidal signal and a corresponding receiving antenna located some distance away. The transmitting antenna generates an electromagnetic field in the electrically conducting earth around the borehole, thereby inducing secondary (induced) currents to flow in the formation. At the receiver end, the measured field includes both primary (generated) and secondary (induced) field components. If the primary field is subtracted from the data, the remaining field (secondary) is a direct indicator of the subsurface electrical conductivity between the source and receiver antennas.

If the antennas are located close together, as is the case in a single-hole logging devise, the tool investigates a relatively small region that is centered adjacent to the borehole (approximately 0.5 m). In this region, it is usually safe to assume that the electrical

conductivity is uniform. The measurements are then converted from electromagnetic field to electrical conductivity using a simple formula for a homogeneous earth.

The cross-borehole technique uses the same principle as the borehole induction log, but the source and receiver antennas are located in separate boreholes. Under these conditions, the measurements are sensitive to the region between the wells. The analysis of collected data is substantially more complex, however, since we cannot assume that the earth is uniform between the boreholes. Data are interpreted using complex numerical models and imaging techniques

If only one borehole is available or if wells are widely separated, then we may apply electromagnetic induction techniques in a surface-to-borehole configuration. With this method, a series of surface-installed loop transmitters are employed together with borehole receiver antennas. In general, the surface-to-borehole method is less sensitive to detailed subsurface conductivity structure than single hole or cross-borehole techniques, but it is more sensitive than surface-based methods.

LLNL/LBNL Field System

The LLNL / LBNL EM field system was developed in 1990 for oil-field characterization and process monitoring (Wilt et al., 1995). It may be deployed in crosshole, surface-to-borehole, and surface configurations and has proven effective from boreholes up to 500 m apart (Figure 4). As with any tomographic system, data are collected by positioning transmitter and receiver tools at several levels that encompass the area of interest between the boreholes. A typical data set consists of several thousand measurements.

The transmitter station generates high-power ac signals at the surface and sends them down standard logging cable to be broadcast using a vertical-axis coil antenna. The transmitter coil consists of a magnetically permeable rod (mu-metal or ferrite) wrapped with several hundreds turns of wire and tuned with capacitors to broadcast a single frequency. Typically the core rod is 2 to 3 m long and 3 to 4 cm in diameter; the strength of the transmitter is proportional to the volume of this core. We can change the frequency by changing the number of turns (inductance) and / or capacitor in the tool. A surface-based loop transmitter is used for the surface-to-borehole system. This transmitter is operated in the same manner as the borehole source (i.e., tuned with capacitors), but because of the large surface area, it is 10 to 100 times more powerful.

Vertical magnetic fields are detected at the receiver borehole with a commercial borehole receiver coil, and the signal is amplified and transmitted up the logging cable for measurement with a lock-in amplifier. The lock-in amplifier operates by measuring magnetic fields that are synchronous with an external phase reference, in this case the transmitter signal. This phase reference is carried from the transmitter to the receiver using an

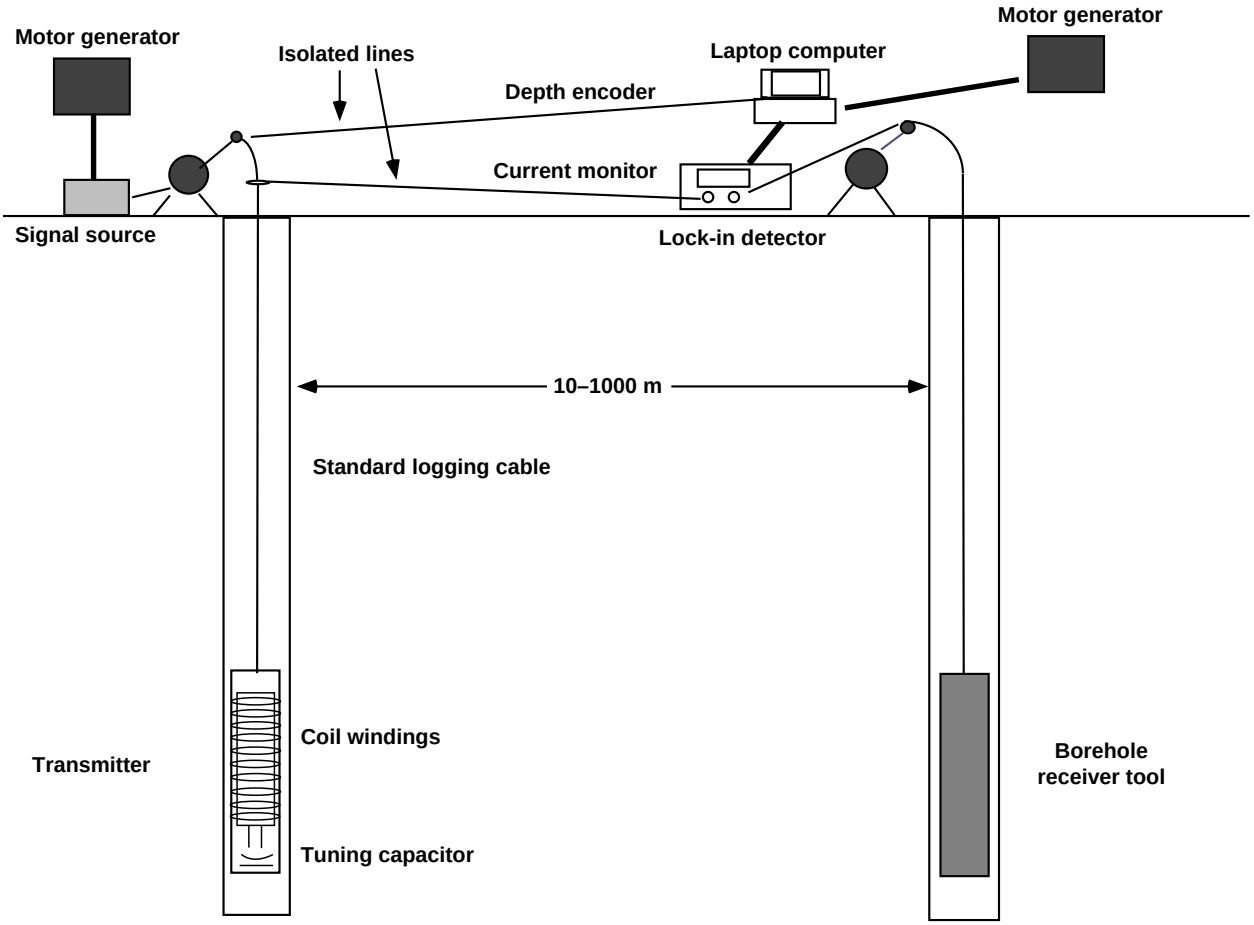

Figure 4. Schematic diagram for the LLNL/LBNL EM system.

optically isolated line. Wheel-type encoders are used to track tool depths, and a portable computer is used to log the data.

With these simple analog systems, we have collected high-quality data at a variety of field sites at borehole separations from 10 to 300 m using frequencies from 100 Hz to 100 kHz (Wilt et al., 1991). Data are typically repeatable and reciprocal to 1%. We believe that the high quality of the data is due to careful attention to isolation and local grounding of the transmitter and receiver sections. Each unit has a separate generator for power supply and a local common ground. The transmitter and receiver modules are connected for phase reference and depth control, using optically isolated cables.

Field data are interpreted using numerical models and regression analysis (inversion) that fit the EM fields to a two- or three-dimensional resistivity distribution. We use a two-dimensional rectangular mesh code, developed at Schlumberger-Doll Research (Torres-Verdin and Habashy, 1993), and a three-dimensional rectangular mesh code developed by Ki Hu Lee of Lawrence Berkeley National Laboratory. Because of the complexity of the

electromagnetic field in a discontinuous medium, a typical data inversion requires more than 12 hours for the two-dimensional solution to more than one day for the three-dimensional code on a fast computer workstation.

For the surface-to-borehole data, we use only a one-dimensional solution at present and piece together the best-fit layered models. Interpretation of these data using two- and three-dimensional models is presently impractical because of the large volumetric coverage. This coverage requires enormous meshes for the numerical models to adequately resolve the subsurface resistivity structure. Numerical codes for interpreting these data are being developed.

Field Plan

Figure 4 is a schematic map of steam pattern 2 at the Lost Hills #3 oil field where we are applying crosshole EM as a pilot test. Two fiberglass-cased observation wells 35W and 35E were drilled along a northeast–southwest profile straddling steam injector #5035. The wells were drilled for the combined purposes of crosshole EM surveys and repeated temperature and induction (resistivity) logging. Steam was injected at depths of 65, 90, and 120 m into upper, middle, and lower members of the Tulare Formation heavy oil sand. Subsurface steam flow is expected to follow the natural northwest–southeast regional strike, with the plume developing as an ellipse having its major axis aligned with the natural fractures. The monitoring wells are positioned orthogonal to the regional strike direction so that the crosshole EM data roughly follow the assumption of a two-dimensional rectangular geometry.

A cross section derived from borehole induction resistivity logs shows that the higher-resistivity intervals (10–100 ohm-m) typically represent the oil sands; the lower-resistivity units (2–10 ohm-m) are associated with confining silts and shales (Figure 5). The target sands extend from 60 to 120 m in three separate intervals. The upper sand is the thickest and most continuous of the three. It lies at a depth of 60 m, has a thickness of up to 20 m, and dips gently eastward at about 6 degrees. The middle and lower members are thinner and less continuous. The middle member is 3 to 6 m thick and is centered at a depth of approximately 90 m. This unit seems to pinch out near well 35W and becomes a water sand somewhere between 35E and borehole 4034. The lower Tulare, centered at a depth of 110 m, is continuous throughout this portion of the field and dips eastward at about 8 degrees. The water table lies at a depth of 160 m, or just below the bottom of these wells.

EM Field Surveys

Crosshole and surface-to-borehole EM data were collected three times: in November 1993, before steam injection began; in April 1994, 6 months after steam injection; and in September 1994, 10 months after injection. Crosshole data were collected at 5 and 20 kHz

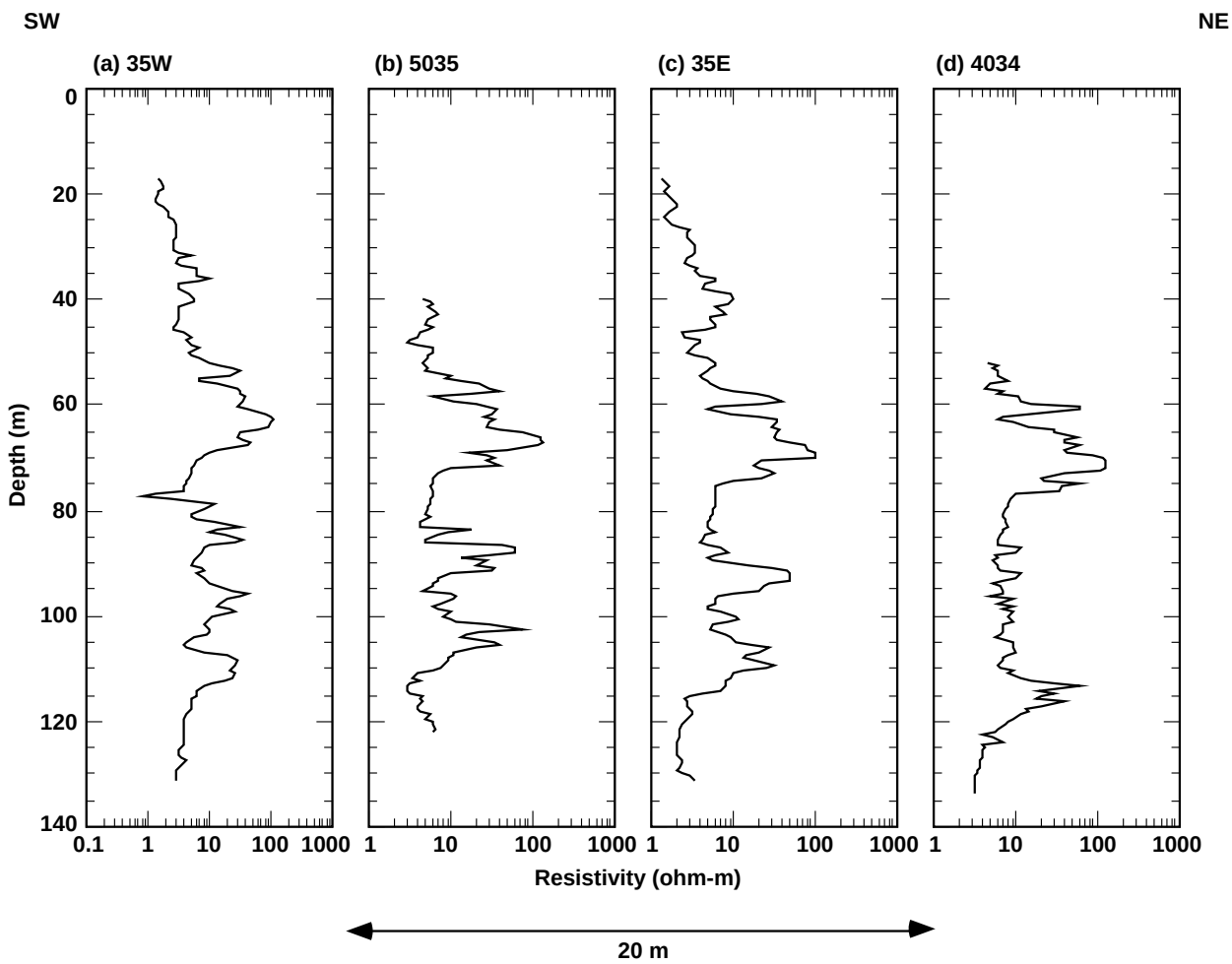

Figure 5. Induction logs along profile A′–A″.

using borehole 35W for the transmitter and 35E for the receiver tool. Receivers were spaced 4 or 8 m apart in borehole 35E, and EM data were collected continuously as the transmitter moved between 130 and 30 m in borehole 35W. A typical crosshole profile required approximately one hour to measure. A typical field survey, which consisted of 18 to 22 profiles, required 20 hours to complete for each frequency.

Surface-to-borehole EM data were collected along profile A′–A″, using 10- × 10-m surface loop transmitting antennas and a borehole receiver antenna. The surface loops are spaced along profile A′–A″ at 10- to 20-m intervals, to a maximum distance of 125 m from the receiver borehole, 35E. For each transmitter, vertical magnetic field data were collected at 6-m intervals at depths from 10 to 140 m using frequencies of 1 and 5 kHz. Individual surface-to-borehole profiles required about one hour; the collection of 16 profiles on line A–A′ required two days for both frequencies.

Crosshole EM Results

Figure 6 shows a sample crosshole EM profile. The profile is measured using a fixed receiver, located within the upper oil sand at a depth of 60 m, and a continuously moving transmitter. Measurements were made at 1-m intervals. At first glance, the amplitude data reflect the relative positions of the source and receiver coils; the fields become larger as the source and receiver coils approach the same level and fall off in proportion to the borehole tool separation. The phase data are considerably more sensitive to the resistivity

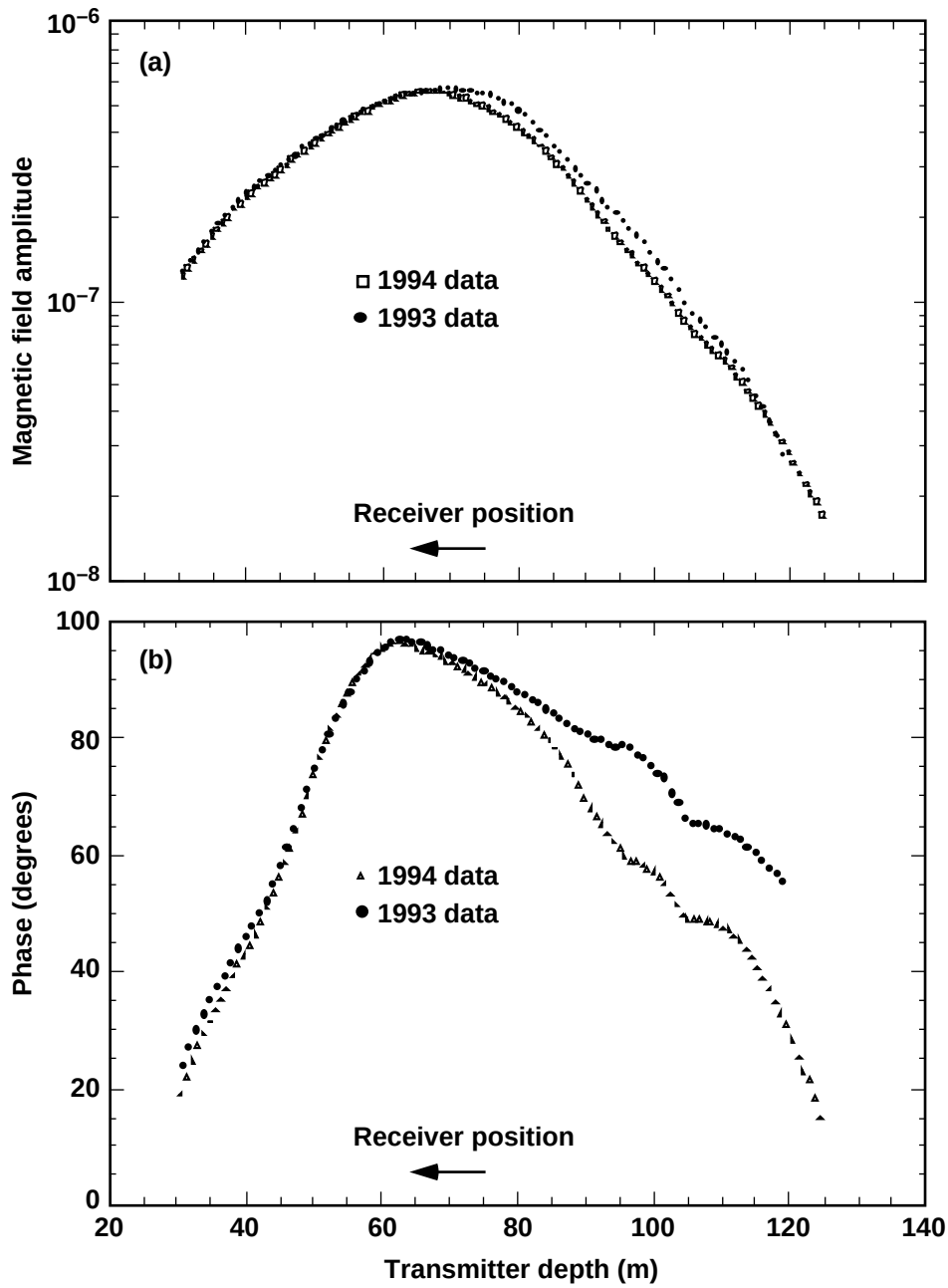

Figure 6. Sample crosshole 5-kHz EM data profiles collected between boreholes 35W and 35E.

distribution. For example, the phases are higher within the higher-resistivity oil strata but show pronounced rotation in the lower-resistivity shale beds above and below the oil sands. The crosshole field data are repeatable to within 2%; we use Figure 6 in estimating data uncertainty during interpretation.

In Figure 7, we show the 5-kHz amplitude and phase data in contoured form for surveys collected before (November 1993) and after (April 1994) steam injection. In general, the contour plots have the same characteristics as the individual profiles; that is, the amplitude data generally reflect the geometric spacing between the borehole tools, while the phase data are maximum in the higher-resistivity oil sands between 60 and 110 m and lower in the low-resistivity silts. Notice that although the data collected in 1993 and 1994 are remarkably similar for tool depths above 60 m, they are quite different below this depth. The data collected in April 1994 show a systematic reduction in both amplitude and phase at depths from 60 to 120 m compared with the November 1993 data. More than a 40% decline in the field amplitude is observed together with a change in the measured phase of more than 20 degrees. We attribute this to decreases in electrical resistivity as a result of the steamflooding. The observed difference in the crosshole data is considerably greater than it is in the surface-to-borehole observations. This is primarily because the crosshole tools are closer to the steamed zone and because a higher frequency is applied in the crosshole surveys.

Crosshole EM data were interpreted using the two-dimensional code described above. We use a smoothed version of the induction resistivity logs in boreholes 35W and 35E as a starting estimate for the inversion, and the computer changed the interwell conductivity distribution until the observed field data match the calculated data to within the observed field error of 2%. For each data set, the code required 20 iterations and approximately 20 hours on an IBM model 590-600 computer workstation to reach a final model.

Figure 8 shows the interpreted subsurface resistivity distribution between boreholes 35E and 35W before and after steam injection. These images represent an interpretation of the three individual data sets collected in 1993 and 1994. The arrows show the steam-injection intervals in injection borehole 5035 and O35. The darker sections of the images represent higher-resistivity zones associated with heavy-oil sands; the lighter areas are lower-resistivity silts and confining shale beds of 2 to 6 ohm-m. The pre-injection image in Figure 8a shows the upper oil sand to be a thick, continuous unit dipping gently eastward. The middle and lower sands are thinner and more discontinuous between the wells. Note that there is a certain amount of blurring in these layers; we believe this blurring is primarily caused by the coarseness of the numerical grid (2×2 m). The images in Figures 8b and 8c are visibly different only at depths below 80 m in the region below the injection borehole. In this portion of the figure, the resistivity has decreased significantly because of the steam injection. In all other parts of the image, the before and after data agree to within a few percent.

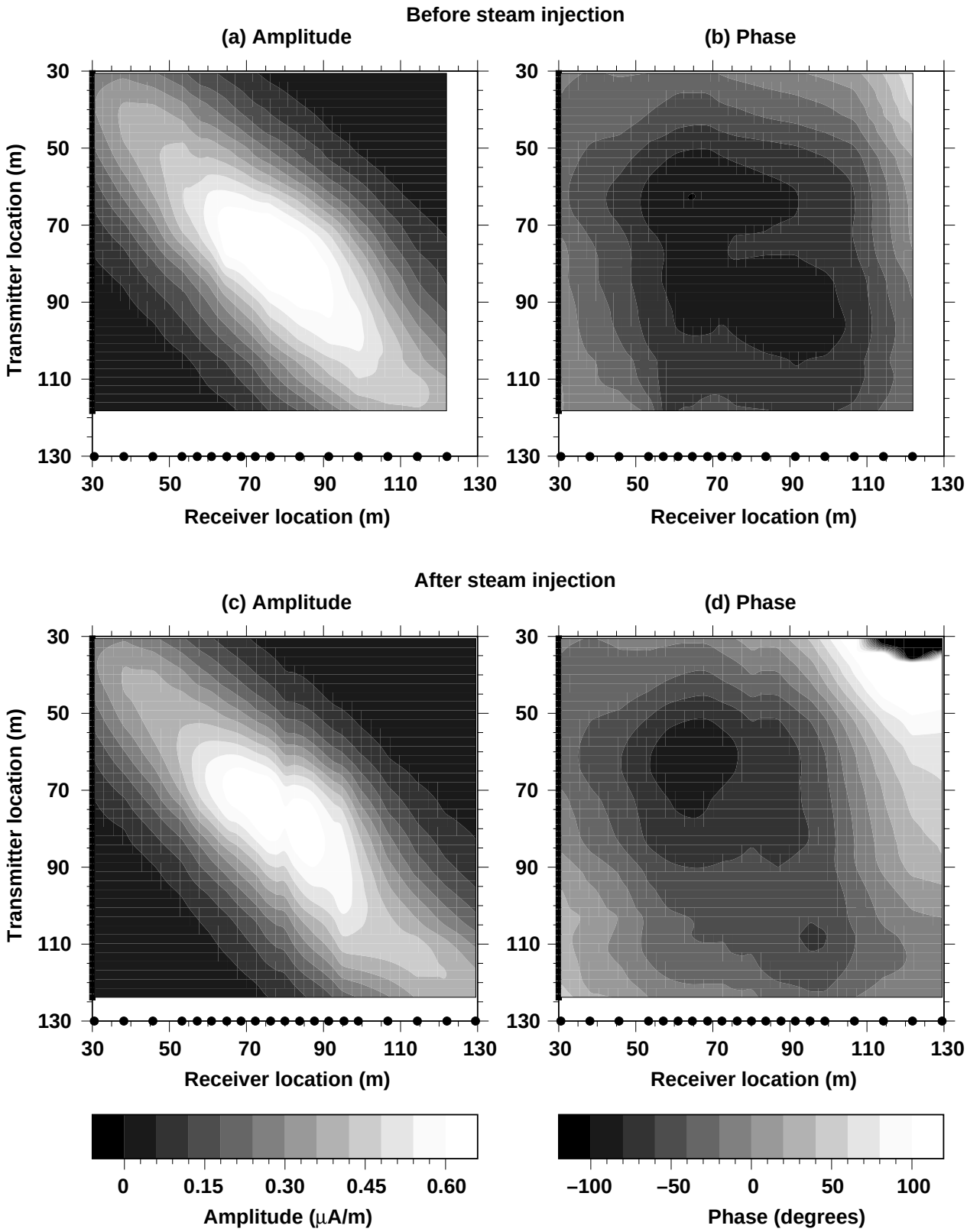

Figure 7. Combined 5-kHz crosshole data set before and six months after steam injection.

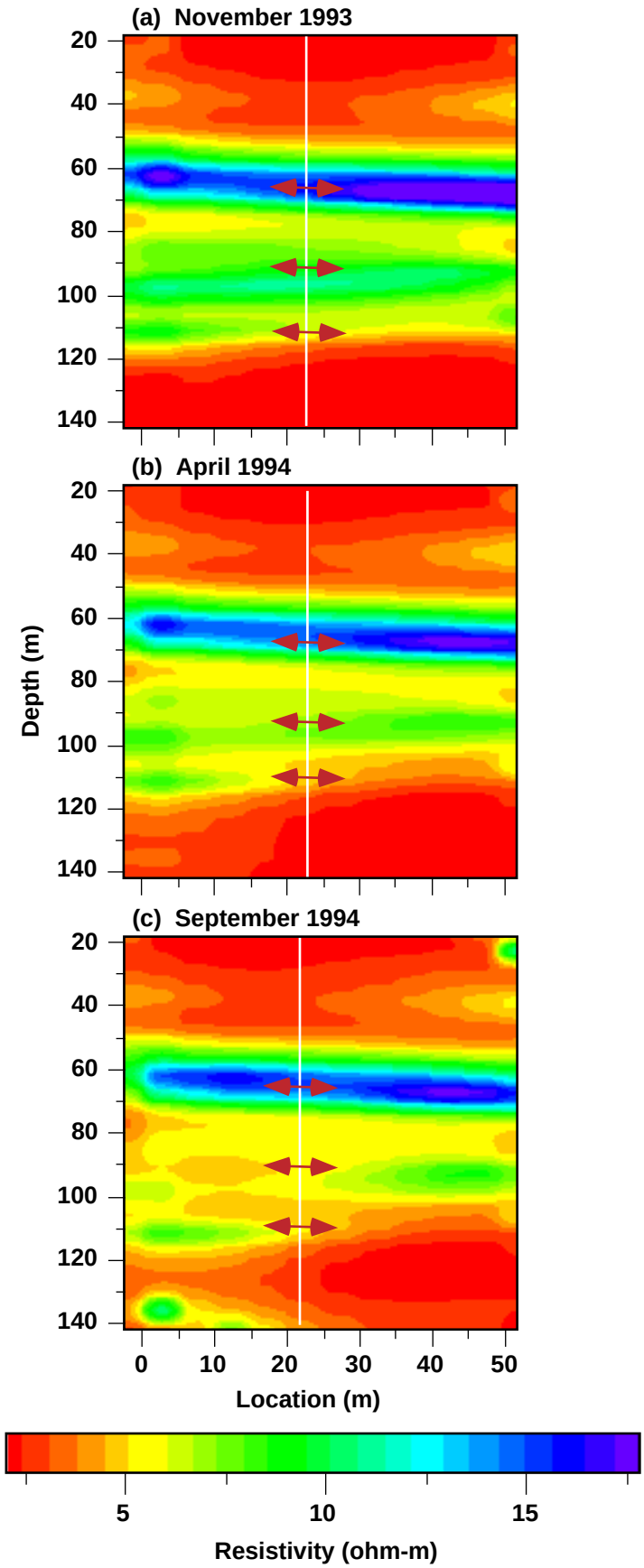

Figure 8. Resistivity images derived from crosshole EM data (a) before steam-flooding, (b) 6 months after flooding, and (c) 10 months after flooding.

In Figure 9, we show two difference images, made by subtracting the baseline images from the two post-steamflood images; again, the arrows represent the steam-injection intervals. The darker portions of these difference images indicate substantial decreases in the subsurface resistivity as a result of the steam injection; the greatest difference is a decrease of more than 35% in the region surrounding the injection hole at depths below 80 m. These images indicate that a substantial steam chest has formed in the middle and lower sands, and almost none of the steam has gone into the upper oil sand. The difference images also show that the injected steam is preferentially moving eastward in the lower oil sand but westward in the middle sand. We note that nearby producer 4034 was not completed in the middle oil sand because on this well site, at the eastern margin of the field, the middle sand is water saturated. The well is therefore providing no eastward pull to the steam, thereby leaving it to respond only to the pressure gradients from the other producers to the west, north, and south. We explain the eastward movement of the steam in the lower Tulare by better stratigraphic connection as noted in the borehole logs shown in Figure 5.

Since steam injection logs in well 5035 show that a considerable amount of steam penetrates in the upper perforated zone, it is unknown why there is no evidence of steam chest formation in the EM results. This may be because the colder and more viscous oil in the thicker upper Tulare sand is responding much more slowly to the steam injection. If so, the steam plume will develop later. Alternatively, there may be a connection from the upper to the lower Tulare sands via natural or man-made fractures. Such a connection would redirect the steam into these lower units. The worst case is that the steam could be filling an upper air-filled sand, which would pose a safety hazard. Since no evidence of this is manifest in the well data or in the surface-to-borehole EM results, our results suggest that, to date, the steam is confined to the oil-bearing strata.

Note that Figure 9 provides only a two-dimensional picture of subsurface steam flow perpendicular to the prevailing northwest–southeast geologic strike. The steam plume is clearly a three-dimensional structure, and in fact, we expect that most of the steam flow will be along geologic strike. If, for example, the plume in the upper oil sand is developing as a very narrow ellipsoid, parallel to geologic strike, it may not be evident on the crosshole data.

In February 1995, Mobil contracted for repeat induction resistivity and temperature logs in borehole 35W to determine if steam breakthrough had occurred; we show these logs together with similar logs made before injection in Figure 10. The temperature logs in Figure 10 confirm that steamflooding has been restricted to the lower two Tulare sands and that the flooding is associated with a substantial resistivity decrease in the high-temperature zones. Well-log resistivity decreased by 30 to 50% in the middle oil sand and the associated confining silts; this decrease is in accord with predictions from the crosshole EM surveys. These changes are in close agreement with observed changes in the South Belridge Tulare sands after steamflooding (Ranganayaki et al., 1992).

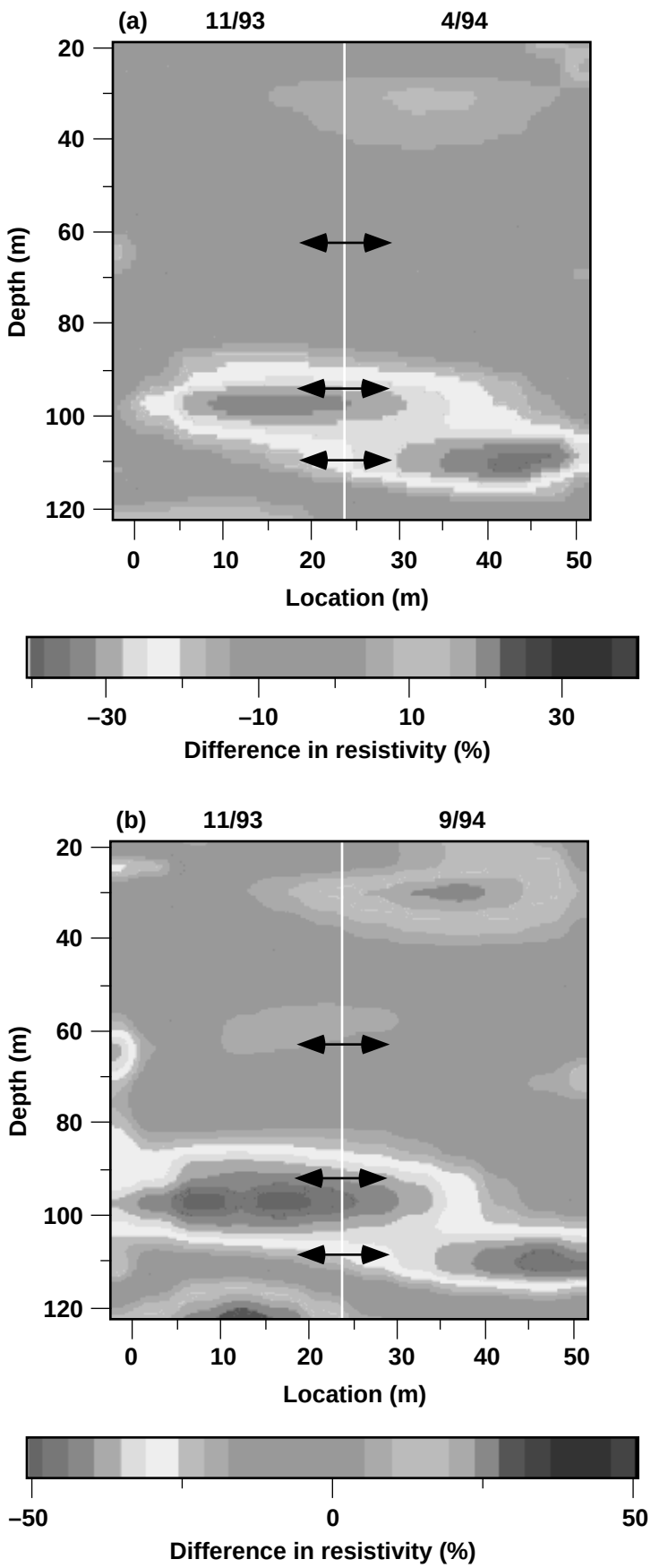

Figure 9. Resistivity difference images of crosshole EM data before steamflooding, 6 months after flooding, and 10 months after flooding. Differences were made by subtracting the baseline image from the postflood images of Figure 8.

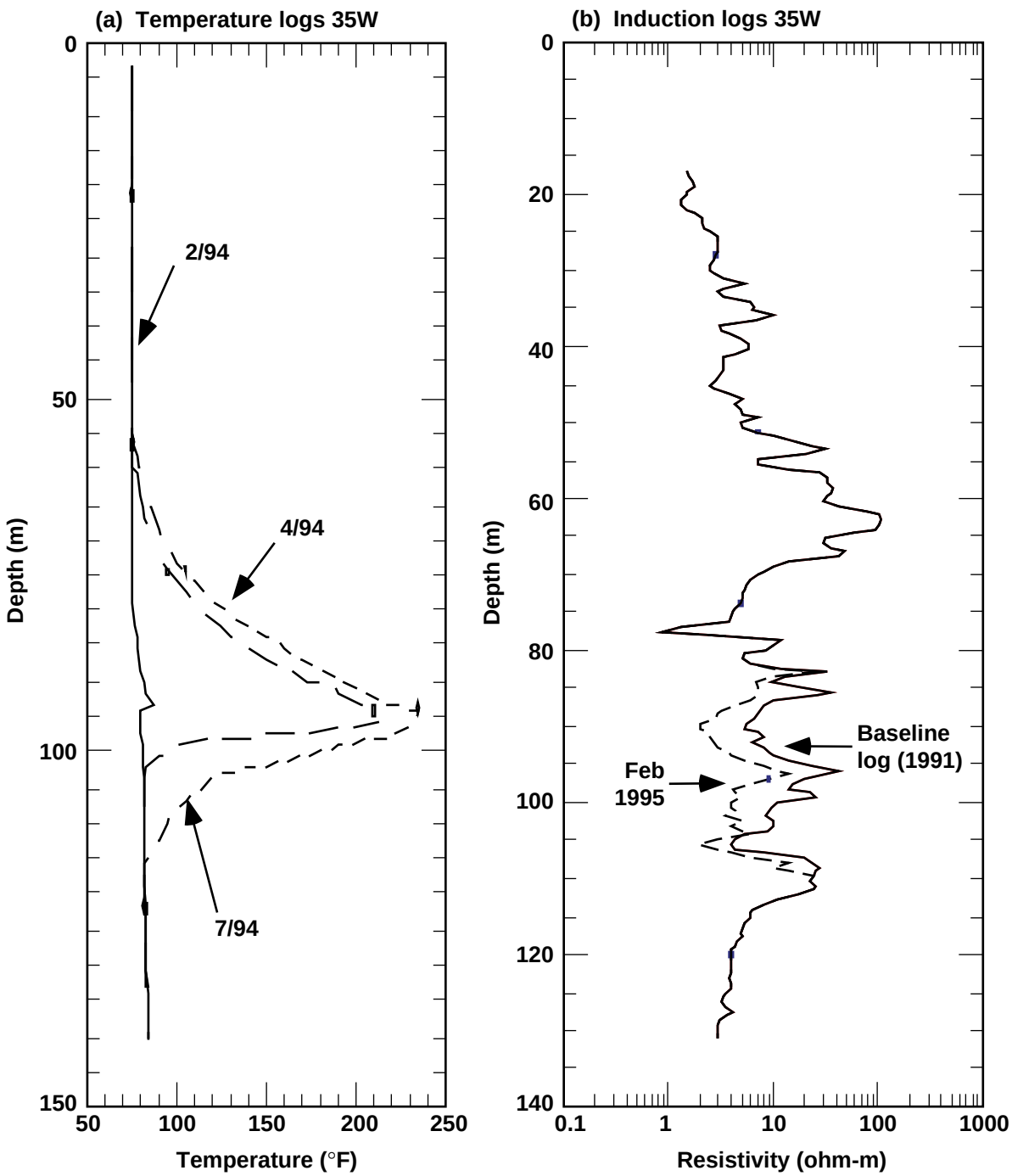

Figure 10. Temperature and induction resistivity well logs collected in borehole 35E before and after steamflooding.

Note that the reduction in resistivity is in accord with expected changes due to temperature alone (Keller, 1988). This is not obvious because the resistivity of sedimentary rock is a complex function of porosity, clay content, fluid type, salinity, and saturation as well as temperature. An earlier analysis of a similar steamflood showed that, although

steam injection results in measureable changes in saturation and fluid salinity, these affects seem to cancel each other and the combined affects on the resistivity of the rock is often quite small (Newmark and Wilt, 1992). In fact, in sands and clays the resistivity changes can be predicted within 10% on the basis of temperature.

Surface-to-Borehole Results

Figure 11 shows a sample surface-to-borehole profile with the fit from the one-dimensional model. The profile shows the 1-kHz EM field amplitude as a function of depth in borehole 35E using a surface loop transmitter located 25 m from the well. The 11-layer, one-dimensional model is made by initially assuming that the earth consists of 12 layers of equal resistivity each 10 m thick. The resistivity of the layers (but not the thicknesses)

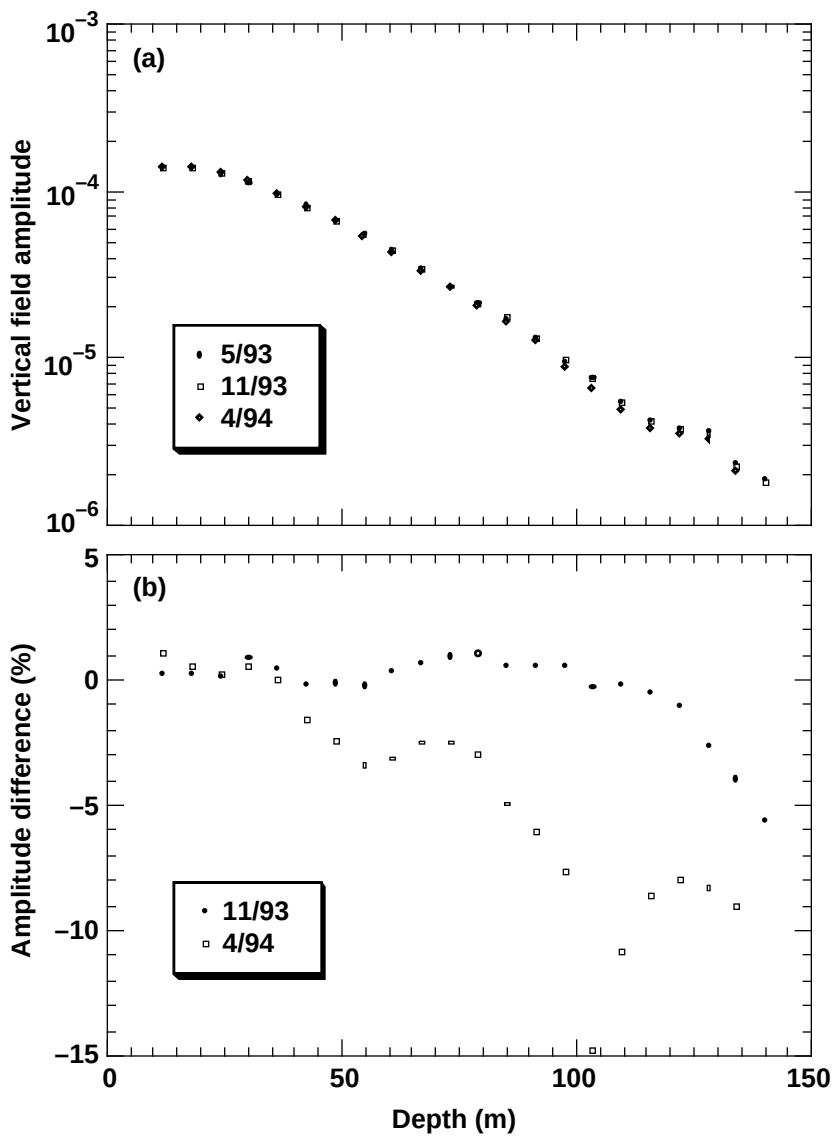

Figure 11. Sample surface-to-borehole data plot.

was then adjusted by the computer until the observed and calculated data match. A similar plot is produced from each of the 16 loop transmitter sites. The layered models derived from the surface-to-borehole data agree well with the borehole induction log, but the lateral structure may not be obtained from the layered models.

In general, the surface-to-borehole data quality was good, with most individual profiles repeating over time from 1–2% for shallow receiver depths to 2–5% for greater depths. The plot in Figure 12 is typical of difference in observed data collected over long time intervals. Notice that the amplitude profiles collected before and after steaming are quite similar at shallow depths but begin to diverge in the lower 20 to 30 m of the well. The later measurements are lower in amplitude, which typically indicates a decrease in resistivity. Although we can reasonably attribute this change as the effects of subsurface steam flow, we found that the observed change is too small and the data were not sufficiently accurate for use in detailed modeling. As the steamflood develops further over time, we expect it to be more visible to these data, but at present, it is difficult to delineate. At the three transmitter sites adjacent to the steam injection well, some of the data show obvious signal contamination probably because of the nearby steam pipes and well casings.

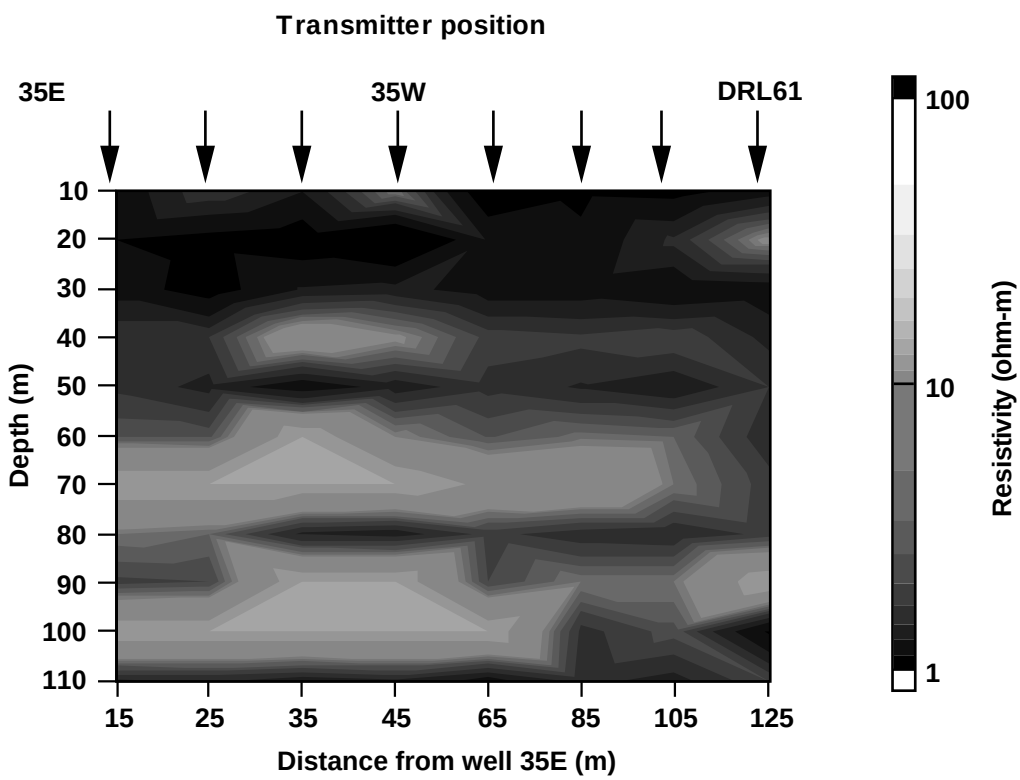

Figure 12. Pieced-together one-dimensional inversion of surface-to-borehole data along A′–A″.

As the steamflood develops further, we expect the surface-to-borehole results to become more and more sensitive to subsurface changes. This is especially true if the steam begins to flow in the shallower upper Tulare sand. Then the technique will offer significant advantages in that we are not restricted to the plane between boreholes and we may deploy our system along any arbitrary profile.

Although data interpretation is at present in a primitive state, several interpretational tools are being developed. The interpretation problem for this configuration is much more difficult than the crosshole case because of the surface layer and because a much greater volume of rock is affected by the measurements.

Discussion and Conclusions

Since it is a pilot for the development of almost 5 million barrels of oil, this project has been given every opportunity to succeed. However, in October 1994, after three years of continuous steam injection, the two western patterns were shut-in due to lack of response. In addition, the shallow steamflood has had eight incidences of steam breaching the ground surface, each resulting in extended periods of non-injection, subsequent steam restrictions, and ultimately, the closure of one pattern.

The upper oil sand is clearly having some difficulty accepting steam, at least in the initial phase of steamflooding. We expect that this unit will also develop a substantial steam chest but it will require more time. We plan to collect crosshole and surface-to-borehole EM data in this area at 6-month to 1-year intervals, so we can continue to monitor the movement of the underground stream. Our modeling results indicate that when substantial steam flow occurs in the upper oil sand, both crosshole and surface-to-borehole data should be able to detect it.

Results from this project have demonstrated that crosshole EM can be a powerful tool in reservoir characterization and process monitoring. This finding is particularly encouraging because the technology is relatively young. We can therefore expect significant improvements in data collection and image definition to be forthcoming. In addition, the method is well suited for joint interpretation with seismic and other data types.

The practical challenge is to incorporate technologies such as crosshole EM and seismics in field monitoring in a cost-effective manner. These technologies serve to improve the knowledge of reservoir geometry and to allow the engineer more control of secondary and tertiary recovery processes.

Acknowledgments

This project was funded by the U.S. Department of Energy through Fossil Energy research under Contract W-7405-Eng-48. We thank project manager Tom Reid for his continued support. We also thank Mike Deets, at Mobil in Bakersfield and Kim Halbert at Lost Hills for their cooperation and support throughout this project. Field technicians Don Lippert and Jim Dougherty, from the Geophysical Measurement Facility at Lawrence Berkeley National Laboratory were instrumental in the data collection.

References

Eastwood, J.; Lebel, P.; Dilay, A.; and Blakeslee, S. (1994), "Seismic Monitoring of Steam-Based Recovery of Bitumen," *The Leading Edge* **13**(4), 242–251.

Keller, G. V. (1988), "Rock and Mineral Properties," in *Electromagnetic Methods in Applied Geophysics, Vol. 1, Theory.* Investigations in Geophysics Series, No. 3 (Society of Exploration Geophysicists, Tulsa, OK), pp. 13–51.

Mansure, A. J.; and Meldau, R. F. (1990), "Steam-Zone Electrical; Characteristics for Geodiagnostic Evaluation of Steamflood Performance," *Soc. Petrol. Eng. Formation Evaluation* September, pp. 241–247.

Miller, D.; McPherson, J. G.; and Covington, T. E. (1990), "Fluvio-Deltaic Reservoir, South Belridge Field, San Joaquin Valley, California," in Barwis, J. H.; McPherson, J. G.; and Studlick, J. R. (Eds.), *Sandstone Petroleum Reservoir* (Springer-Verlag, New York, NY), pp. 109–130.

Newmark, R., and Wilt, M. J. (1992), "Changes in Formation Electrical Properties during Steam Flooding," *Expanded Abstacts, Soc. Explor. Geophys. Annual Meeting* (New Orleans, LA), pp. 488–491.

Ranganayaki, R. P.; Akturk, S. E.; and Fryer, S. M. (1992), "Formation Resistivity Variation due to Steam Flooding: A Log Study," *Geophys.* **57**(3), 488–494.

Spies, B. R.; and Greaves, R. J. (1990), "Numerical Modeling of Surface-to-Borehole Electromagnetic Surveys for Monitoring Thermal Enhanced Oil Recovery," *Geoexploration* **60**(9)**.**

Torres-Verdin, C.; and Habashy, T. (1993), "An Approach to Nonlinear Inversion with Application to Cross-Well EM Tomography," in *Extended Abstracts Society of Exploration Geophysicists Annual Meeting,* pp. 351–354.

Wilt, M. J.; Morrison, H. F.; Becker, A.; and Lee, K. H. (1991), *Cross-Borehole and Surface-to-Borehole Electromagnetic Induction for Reservoir Characterization*, U.S. Department of Energy, Washington, DC, DOE/BC/91002253.

Wilt, M. J.; Alumbaugh, D. L.; Morrison, H. F.; Becker, A.; Lee, K. H.; and Dezcz-Pan, M. (1995), "Crosswell Electromagnetic Tomography: System Design Considerations and Field Results," *Geophys.* **60**(3), 871–885.